Automatic one-loop calculations with Sherpa+OpenLoops

F Cascioli[1]**, S Höche**[2]**, F Krauss**[3]**, P Maierhöfer**[1,†]**, S Pozzorini**[1] **and F Siegert**[4]

[1] Institut für Theoretische Physik, Universität Zürich, 8057 Zürich, Switzerland
[2] SLAC National Accelerator Laboratory, Menlo Park, CA 94025, USA
[3] Institute for Particle Physics Phenomenology, Durham University, Durham DH1 3LE, UK
[4] Physikalisches Institut, Albert-Ludwigs-Universität Freiburg, D-79104 Freiburg, Germany

E-mail: `cascioli@physik.uzh.ch`, `shoeche@slac.stanford.edu`, `frank.krauss@durham.ac.uk`, `philipp@physik.uzh.ch`, `pozzorin@physik.uzh.ch`, `frank.siegert@cern.ch`

Abstract. We report on the `OpenLoops` generator for one-loop matrix elements and its application to four-lepton production in association with up to one jet. The open loops algorithm uses a numerical recursion to construct the numerator of one-loop Feynman diagrams as functions of the loop momentum. In combination with tensor integrals this results in a highly efficient and numerically stable matrix element generator. In order to obtain a fully automated setup for the simulation of next-to-leading order scattering processes we interfaced `OpenLoops` to the `Sherpa` Monte Carlo event generator.

1. Introduction

The simulation of multi-particle scattering amplitudes with next-to-leading order (NLO) accuracy is a key requirement for the analysis of the data taken at the Large Hadron Collider. The necessity to manage the large number of processes to be considered at the experiments demands for integrated frameworks which automate the full tool-chain from the matrix element generation to hadronic final states via Monte Carlo event generators.

Regarding the NLO matrix elements, in the last few years the approach based on tensor integral reduction and algebraic methods was pushed to processes which involve up to 6 external particles [1, 2]. While this method can lead to efficient code its applicability is limited by expensive algebraic simplifications and the size of the process specific code. On the other hand the application of on-shell reduction techniques e. g. in combination with tree-level recursions lead to a high degree of automation of one-loop generators [3–8].

The open loops algorithm [9] exhibits a new way to calculate loop amplitudes using a tree-like recursion for loop momentum polynomials [10] and tensor integrals. The algorithm can be fully automated and achieves high efficiency and numerical stability. A generator based on a similar approach with a Dyson-Schwinger recursion and tensor integrals was presented in [11].

†Speaker; talk given at the International Workshop on Advanced Computing and Analysis Techniques in Physics Research (ACAT), Beijing, China, May 2013.

We interfaced our `OpenLoops` implementation [9] to `Sherpa` [12] which provides us with Monte Carlo integration, MC@NLO matching [13–15] to the `Sherpa` parton shower and MEPS@NLO multi-jet merging [16, 17]. Within this framework we calculated QCD corrections to four lepton production as a background to $\mathrm{H} \to \mathrm{WW}^* \to \ell\nu\ell\nu$ [18]. After the discovery of the Higgs boson [19, 20] this channel continues to play an important role in the investigation of its properties. To render the signal visible it is necessary to apply jet vetoes and perform the analysis in exclusive jet bins, in particular to suppress the background due to $\mathrm{t}\bar{\mathrm{t}}$ production. The MEPS@NLO method allows us to retain NLO accuracy in the individual jet bins and resum potentially large logarithms.

The production of two W-bosons including leptonic decays was studied extensively in the literature [21–26] and also matched to parton showers with the MC@NLO [13] and with the POWHEG method [27, 28]. W-pair production in association with a jet [29–31] has been studied as well, however previously to our simulation not matched to a parton shower.

In section 2 we recapitulate the open loops algorithm and in section 3 we introduce the `Sherpa`+`OpenLoops` framework. Results for the four lepton production are shown in section 4.

2. The open loops algorithm and its implementation in `OpenLoops`

Tree-level amplitudes $\mathcal{M}$ and one-loop corrections $\delta\mathcal{M}$ are handled as sums of tree and one-loop Feynman diagrams,

$$\mathcal{M} = \sum_d \mathcal{M}^{(d)}, \qquad \delta\mathcal{M} = \sum_d \delta\mathcal{M}^{(d)}, \tag{1}$$

allowing for the factorisation of colour factors from the Lorentz structure of the diagrams. This way the colour reduction can be done once per process, resulting in negligible CPU cost for the colour summation [32].

Colour stripped tree diagrams are calculated by recursively connecting "sub-trees" starting from external wave functions. A sub-tree which is obtained from a tree diagram by cutting a line is represented as a complex n-tuple $w^\beta(i)$, where β is the spinor or Lorentz index of the cut propagator and the index i represents the topology, (off-shell) momentum, and particle content,

$w^\beta(i) =$ 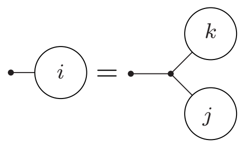 . (2)

Cut lines are marked by dots, and external lines are not depicted. For brevity, quartic vertices are not shown explicitly, but their inclusion is straightforward. In terms of n-tuples, the recursion step reads

$$w^\beta(i) = \frac{X^\beta_{\gamma\delta}(i,j,k)\; w^\gamma(j)\; w^\delta(k)}{p_i^2 - m_i^2 + \mathrm{i}\varepsilon}, \tag{3}$$

where $X^\beta_{\gamma\delta}/(p_i^2 - m_i^2 + \mathrm{i}\varepsilon)$ describes a vertex connecting i, j, k, and a propagator attached to i. The recursion terminates when the sub-trees which are needed to build all tree diagrams have been generated. Sub-trees which appear in more than one diagram are calculated once and used in all occurrences. The numerical implementation of the algorithm is based on universal routines which implement all wave functions, propagators and vertices corresponding to the Feynman rules of the theoretical model.

A colour stripped n-point one-loop diagram $\delta\mathcal{A}^{(d)}$ is regarded as an ordered set of n sub-trees, $\mathcal{I}_n = \{i_1, \ldots, i_n\}$, connected by loop propagators,

$$\delta\mathcal{A}^{(d)} = \int \frac{\mathrm{d}^D q \, \mathcal{N}(\mathcal{I}_n; q)}{D_0 D_1 \ldots D_{n-1}} = \tag{4}$$

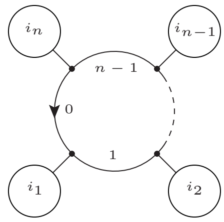

The denominators $D_i = (q + p_i)^2 - m_i^2 + \mathrm{i}\varepsilon$ depend on the loop momentum q, external momenta p_i, and internal masses m_i. All other contributions from loop propagators, vertices, and external sub-trees are summarised in the numerator, which is a polynomial of degree $R \le n$ in the loop momentum,

$$\mathcal{N}(\mathcal{I}_n; q) = \sum_{r=0}^{R} \mathcal{N}_{\mu_1 \ldots \mu_r}(\mathcal{I}_n) \, q^{\mu_1} \ldots q^{\mu_r}. \tag{5}$$

Momentum-shift ambiguities are eliminated by setting $p_0 = 0$, singling out the D_0 propagator. The loop momentum q flowing through this propagator is marked by an arrow in (4). After cutting the D_0 propagator the numerator function can be constructed by recursively attaching sub-trees to the loop

$$\mathcal{N}_\alpha^\beta(\mathcal{I}_n; q) = \tag{6}$$

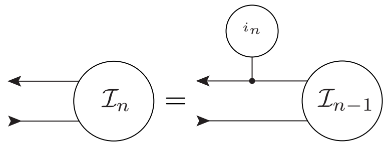

The indices α, β stand for the spinor rsp. Lorentz indices of the cut propagator. Analogously to eq. (3) the numerator $\mathcal{N}_\alpha^\beta$ is built by recursively attaching sub-trees,

$$\mathcal{N}_\alpha^\beta(\mathcal{I}_n; q) = X_{\gamma\delta}^\beta(\mathcal{I}_n, i_n, \mathcal{I}_{n-1}) \, \mathcal{N}_\alpha^\gamma(\mathcal{I}_{n-1}; q) \, w^\delta(i_n), \tag{7}$$

where $X_{\gamma\delta}^\beta$ are the same vertices as in the tree recursion. Separating the loop momentum from its coefficients

$$\mathcal{N}_\alpha^\beta(\mathcal{I}_n; q) = \sum_{r=0}^{R} \mathcal{N}_{\mu_1 \ldots \mu_r; \alpha}^\beta(\mathcal{I}_n) \, q^{\mu_1} \ldots q^{\mu_r}, \quad X_{\gamma\delta}^\beta = Y_{\gamma\delta}^\beta + Z_{\mu;\gamma\delta}^\beta q^\mu \tag{8}$$

leads to a recursion relation for the so-called open loops which encode the functional dependence of the numerator on the loop momentum

$$\mathcal{N}_{\mu_1 \ldots \mu_r; \alpha}^\beta(\mathcal{I}_n) = \left[Y_{\gamma\delta}^\beta \, \mathcal{N}_{\mu_1 \ldots \mu_r; \alpha}^\gamma(\mathcal{I}_{n-1}) + Z_{\mu_1;\gamma\delta}^\beta \, \mathcal{N}_{\mu_2 \ldots \mu_r; \alpha}^\gamma(\mathcal{I}_{n-1}) \right] w^\delta(i_n). \tag{9}$$

The recursion terminates with the contraction of the α, β indices $\mathcal{N}_{\mu_1 \ldots \mu_r} = \mathcal{N}_{\mu_1 \ldots \mu_r; \alpha}^\alpha$, resulting in the coefficients of the tensor integral representation of the diagram

$$\delta\mathcal{A}^{(d)} = \sum_{r=0}^{R} \mathcal{N}_{\mu_1 \ldots \mu_r}(\mathcal{I}_n) \, T_{n,r}^{\mu_1 \ldots \mu_r} \quad \text{with} \quad T_{n,r}^{\mu_1 \ldots \mu_r} = \int \frac{\mathrm{d}^D q \, q^{\mu_1} \ldots q^{\mu_r}}{D_0 D_1 \ldots D_{n-1}}. \tag{10}$$

Table 1. Processes which are available to the ATLAS and CMS Monte Carlo working groups. Vector boson production ($V = \mathrm{Z/W^{\pm}}$) includes leptonic decays except for VVV. Lower jet multiplicities are implicitly understood. Brackets denote that the process will be available with the next update.

W/Z	γ	jets	HQ pairs	single-top	Higgs
$V+3j$	$\gamma+3j$	$3(4)j$	$t\bar{t}+1j$	$tb+1j$	$(H+2j)$
$VV+1(2)j$	$\gamma\gamma+1(2)j$		$t\bar{t}V+0(1)j$	$t+1(2)j$	$VH+1j$
$gg\to VV+1j$	$V\gamma+1(2)j$		$b\bar{b}V+0(1)j$	$tW+0(1)j$	$t\bar{t}H$
$VVV+0(1)j$					$qq\to Hqq+0(1)j$

The tensor integrals $T^{\mu_1\ldots\mu_r}_{n,r}$ are subsequently reduced to m-point scalar integrals $T_{m,0}$ with $m = 1,2,3,4$. Alternatively, the OPP method [33] avoids tensor integrals through a direct connection between the numerator $\mathcal{N}(\mathcal{I}_n;q)$ and the scalar-integral representation of the amplitude. The coefficients of the scalar integrals are determined by multiple evaluations of $\mathcal{N}(\mathcal{I}_n;q)$ for loop momenta q which satisfy multiple-cut conditions of the form $D_i = D_j = \cdots = 0$.

We implemented the described algorithm in the program `OpenLoops`, a fully automatic generator for QCD corrections to Standard Model processes. Feynman diagrams are generated by `FeynArts` [34] and `Mathematica` organises the open loops recursion and generates `Fortran 90` code. For the reduction of the tensor integrals we use the `Collier` [35] library which implements the Denner-Dittmaier reduction procedure [36, 37] and the scalar integrals of ref. [38]. The `Collier` library cures numerical instabilities which arise due to vanishing Gram determinants and other kinematic quantities by applying expansions in these quantities, thus allowing for the numerically stable evaluation of tensor integrals in double precision.

Rational terms of type R_2 are reconstructed by counterterm-like Feynman rules [39]. In order to asses the performance and the numerical stability we considered the $2 \to 2,3,4$ reactions $\mathrm{u\bar{u}} \to \mathrm{W^+W^-}+n\mathrm{g}$, $\mathrm{u\bar{d}} \to \mathrm{W^+g}+n\mathrm{g}$, $\mathrm{u\bar{u}} \to \mathrm{t\bar{t}}+n\mathrm{g}$, and $\mathrm{gg} \to \mathrm{t\bar{t}}+n\mathrm{g}$, with $n = 0,1,2$ gluons [9]. For the most complicated $2 \to 4$ processes the runtime per phase space point is below 1 second on an i5-750 CPU (single core) and the size of a compiled process library is of the order of at most 1 MB. The average number of correct digits ranges from 11 to 15 for the 12 processes and the probability to encounter numerical precision below 10^{-5} and 10^{-3} is less than 2 and 0.1, respectively.

3. NLO simulations with Sherpa+OpenLoops

For realistic simulations of NLO processes the matrix elements must be combined with parton showers and hadronisation. Especially for the description of exclusive observables the resummation of large logarithms as provided by a parton shower is imperative.

We wrote an interface to the `Sherpa` Monte Carlo event generator which provides us with Monte Carlo integration, infra-red subtraction, real corrections, MC@NLO matching to its parton shower and MEPS@NLO merging of different jet multiplicities, providing NLO plus parton shower accuracy in the individual jet bins. The interface works in a fully automatic way, loading process libraries on request at runtime. The matrix element generation is steered by standard `Sherpa` runcards.

The `Sherpa`+`OpenLoops` framework is available to the Monte Carlo working groups of the ATLAS and CMS collaborations, including the set of processes shown in table 1. All provided processes were thoroughly validated against an independent in-house matrix element generator.

Apart from the 4 lepton study the framework was applied to $\mathrm{t\bar{t}b\bar{b}}$ production with massive

Table 2. Exclusive 0- and 1-jet bin $\mu^+\nu_\mu e^-\bar{\nu}_e$+jets cross sections in the signal (S) and control (C) regions of the ATLAS analysis at 8 TeV. Fixed-order NLO results are compared to MC@NLO and MEPS@NLO predictions. Scale uncertainties are shown as $\sigma \pm \delta_{\rm QCD} \pm \delta_{\rm res}$, where $\delta_{\rm QCD}$ and $\delta_{\rm res}$ correspond to variations of the QCD ($\mu_{\rm R}, \mu_{\rm F}$) and resummation (μ_Q) scales, respectively. Statistical errors are given in parenthesis.

0-jet bin	NLO $4\ell(+1j)$	MC@NLO $4\ell(+1j)$	MEPS@NLO $4\ell(+1j)$
σ_S [fb]	$34.28(9)\,^{+2.1\%}_{-1.6\%}$	$32.52(8)\,^{+2.1\%}_{-0.8\%}\,^{+1.2\%}_{-0.7\%}$	$33.81(12)\,^{+1.4\%}_{-2.2\%}\,^{+2.0\%}_{-0.4\%}$
σ_C [fb]	$55.76(9)\,^{+2.0\%}_{-1.7\%}$	$52.28(9)\,^{+1.4\%}_{-0.7\%}\,^{+1.4\%}_{-1.1\%}$	$54.18(15)\,^{+1.4\%}_{-1.9\%}\,^{+2.5\%}_{-0.4\%}$
1-jet bin	**NLO $4\ell(+1j)$**	**MC@NLO $4\ell(+1j)$**	**MEPS@NLO $4\ell(+1j)$**
σ_S [fb]	$8.99(4)\,^{+4.9\%}_{-9.5\%}$	$8.02(4)\,^{+8.5\%}_{-6.4\%}\,^{+0\%}_{-3.1\%}$	$9.37(9)\,^{+2.6\%}_{-2.7\%}\,^{+2.5\%}_{-0.0\%}$
σ_C [fb]	$26.50(8)\,^{+6.4\%}_{-12.5\%}$	$24.58(8)\,^{+6.1\%}_{-6.5\%}\,^{+1.2\%}_{-3.0\%}$	$28.32(13)\,^{+3.1\%}_{-4.7\%}\,^{+4.1\%}_{-0.0\%}$

b quarks, matched to the parton shower [40].

4. Irreducible background to H → WW*

We used `Sherpa+OpenLoops`§ for the simulation of $\mu^+\nu_\mu e^-\bar{\nu}_e(+j)$ production (in the following referred to as 4 leptons or $4\ell(+j)$) as irreducible background to $H \to WW^*$ at a centre-of-mass energy of 8 TeV, including off-shell and non-resonant contributions and all respective interferences [18]. To assess the effects of the parton shower and the merging we calculated the processes in three different approximations, fixed order NLO, MC@NLO, and MEPS@NLO.

As input parameters we use

$$M_{\rm W} = 80.399\,{\rm GeV}, \quad M_{\rm Z} = 91.1876\,{\rm GeV}, \quad \Gamma_{\rm W} = 2.0997\,{\rm GeV}, \quad \Gamma_{\rm Z} = 2.5097\,{\rm GeV} \qquad (11)$$

for the vector boson masses and widths. The electroweak mixing angle is obtained from the complex W- and Z-boson masses [41] as

$$\cos^2\theta_{\rm w} = \frac{M_{\rm W}^2 - {\rm i}\Gamma_{\rm W}M_{\rm W}}{M_{\rm Z}^2 - {\rm i}\Gamma_{\rm Z}M_{\rm Z}}, \qquad (12)$$

and the electromagnetic fine-structure constant is derived from the Fermi constant $G_\mu = 1.16637 \cdot 10^{-5}\,{\rm GeV}^{-2}$ in the G_μ-scheme as

$$\alpha^{-1} = \frac{\pi}{\sqrt{2}\,G_\mu M_{\rm W}^2}\left(1 - \frac{M_{\rm W}^2}{M_{\rm Z}^2}\right)^{-1} = 132.348905\,. \qquad (13)$$

As for the parton distribution functions we chose five-flavour CT10 NLO [42] with the respective running strong coupling α_S. To avoid any overlap with $t\bar{t}$ production, only partonic channels without external b quarks are considered. This requires a prescription to separate $W^+W^- + j$ from top pair and single top production which treats infrared singularities and large logarithms arising from $g \to b\bar{b}$ splittings in a well defined way [18]. Such a prescription is not unique and reflects in an ambiguity of the order of 1% which disappears when $W^+W^- + j$ and $W^+W^-b\bar{b}$ are consistently merged.

§Results were obtained with a pre-release version of `Sherpa 2.0` corresponding to SVN revision 21825.

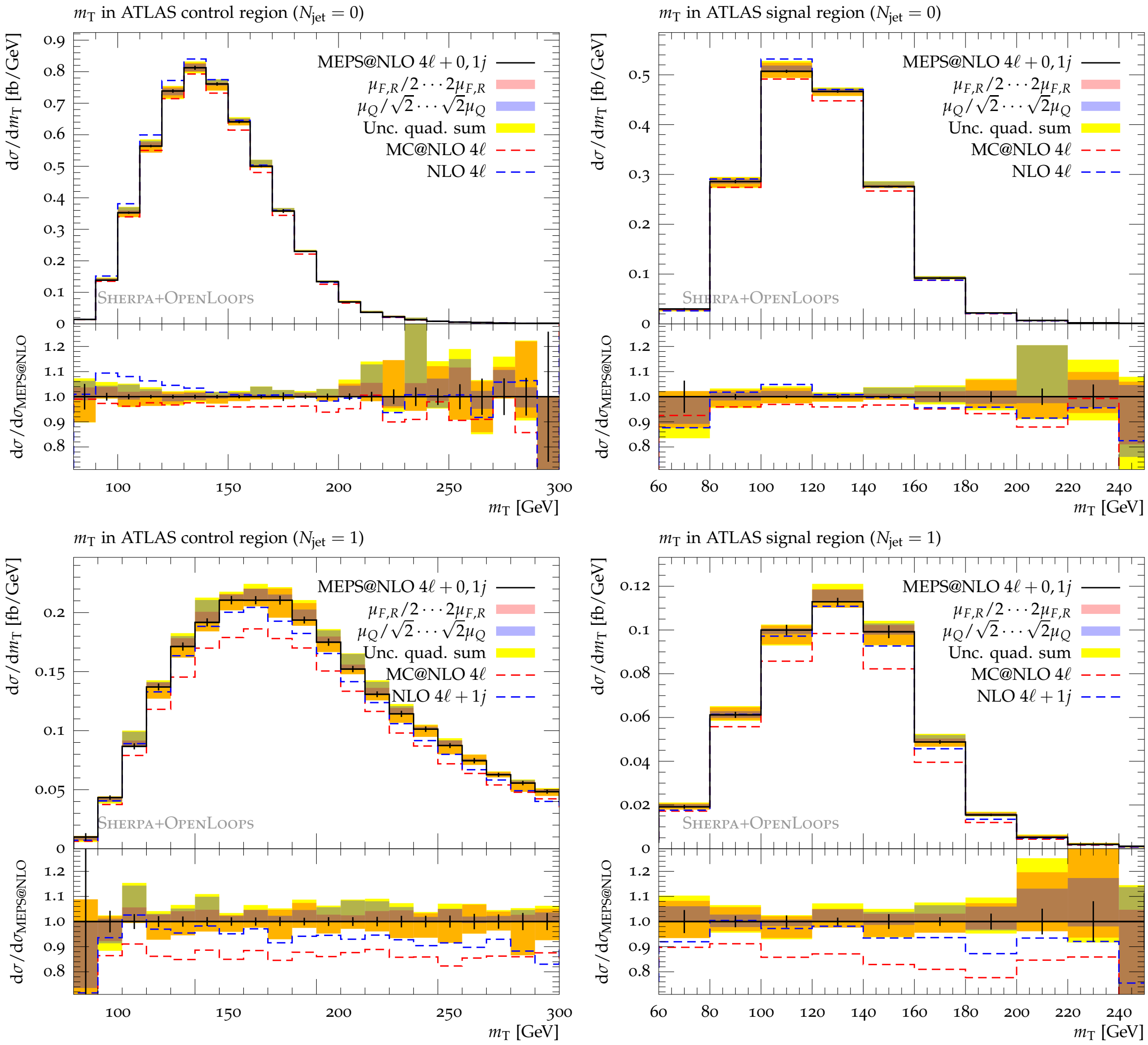

Figure 1. Transverse mass distributions for the ATLAS analysis at 8 TeV after control (left) and signal (right) cuts in the 0-jet (top) and 1-jet (bottom) bins. The lines show MEPS@NLO results (black solid), MC@NLO (red dashed) and NLO (blue dashed) with error bands for μ_R and μ_F factor 2 variations (red) and μ_Q factor $\sqrt{2}$ variations (blue), and quadratically added errors (yellow). Error bands are colour additive (yellow+blue=green, yellow+red=orange, yellow+red+blue=brown).

Table 2 shows the cross sections for the three different simulations in the signal and control regions of the ATLAS analysis. Corresponding results for the CMS analysis can be found in [18]. The default renormalisation (μ_R), factorisation (μ_F) and resummation (μ_Q) scale is chosen as the average transverse energy of the W bosons,

$$\mu_0 = \frac{1}{2}\left(E_{T,\mathrm{W}^+} + E_{T,\mathrm{W}^-}\right), \quad \text{where} \quad E_{T,\mathrm{W}}^2 = M_{\mathrm{W}}^2 + (\vec{p}_{T,\ell} + \vec{p}_{T,\nu})^2. \tag{14}$$

QCD scale uncertainties are estimated by factor 2 variations of μ_R and μ_F, excluding opposite direction variations. The resummation scale μ_Q is varied by a factor $\sqrt{2}$. In the parton shower and for the jet emission in the $4\ell + j$ matrix elements for the MEPS@NLO simulation the scale choice is based on the CKKW technique which adapts the α_S scale to the transverse momentum of the jet. The merging scale Q_{cut} is set to 20 GeV. Figure 1 shows the m_T distributions in the 0- and 1-jet bin in the signal and control regions as defined by ATLAS.

The NLO and MEPS@NLO results agree fairly well with sizeable deviations only in the large m_T region in the 1-jet bin. The good agreement suggests that resummation effects are rather small. The discrepancies between MC@NLO and MEPS@NLO however reach up to 20% in the 1-jet bin with moderate shape distortions. This is not surprising given that the jet emission in the MC@NLO simulation is only leading order accurate.

In the full analysis [18] we also study squared quark-loop contributions which form a finite and gauge invariant subset of NNLO corrections and can have sizeable impact due to opening gluon fusion channels, especially with signal cuts applied. Furthermore several other observables relevant for the experimental analysis are considered as well as the impact of the different approximations on the description of jet veto effects.

5. Conclusions

We implemented a fully automatic generator for NLO QCD corrections to Standard Model processes based on the open loops algorithm to construct loop momentum polynomials by a numerical recursion. With its high performance and numerical stability it is suited to address problems which involve a large number of multi-leg partonic processes. The matrix element generator was interfaced to `Sherpa` and a library for a large set of processes is available to the ATLAS and CMS Monte Carlo working groups.

Within the `Sherpa`+`OpenLoops` framework we performed detailed simulations of the production of 4 leptons with up to one jet as a background for the H $\rightarrow$ WW* analysis of the ATLAS and CMS experiments and studied the impact of parton shower and merging effects. The MEPS@NLO simulation which provides NLO accuracy and resummation in both jet bins is our best prediction and exhibits scale uncertainties below 5%. This approach is particularly suited to study exclusive observables and provides more realistic error estimates.

Acknowledgments

The research of F. Cascioli, P. Maierhöfer and S. Pozzorini was supported by the SNSF. Stefan Höche was supported by the U.S. Department of Energy under Contract No. DE–AC02–76SF00515. Frank Siegert's work was supported by the German Research Foundation (DFG) via grant DI 784/2-1.

References

[1] Bredenstein A, Denner A, Dittmaier A and Pozzorini A 2009 *Phys. Rev. Lett.* **103** 012002 (*Preprint* arXiv:0905.0110 [hep-ph])
[2] Denner A, Dittmaier S, Kallweit S and Pozzorini S 2011 *Phys. Rev. Lett.* **106** 052001 (*Preprint* arXiv:1012.3975 [hep-ph])
[3] Berger C F, Bern Z, Dixon L J, Febres F Cordero, Forde D, Ita H, Kosower D A and Maitre D 2008 *Phys. Rev.* D **78** 036003 (*Preprint* arXiv:0803.4180 [hep-ph])
[4] Ellis R K, Giele W T, Kunszt Z and Melnikov K 2009 *Nucl. Phys.* B **822** 270 (*Preprint* arXiv:0806.3467 [hep-ph])
[5] Hirschi V, Frederix R, Frixione S, Garzelli M V, Maltoni F and Pittau R 2011 *JHEP* **1105** 044 (*Preprint* arXiv:1103.0621 [hep-ph])
[6] Cullen G, Greiner N, Heinrich G, Luisoni G, Mastrolia P, Ossola G, Reiter T and Tramontano F 2012 *Eur. Phys. J.* C **72** 1889 (*Preprint* arXiv:1111.2034 [hep-ph])
[7] Bevilacqua G, Czakon M, Garzelli M V, van Hameren A, Kardos A, Papadopoulos C G, Pittau R and Worek M 2013 *Comput. Phys. Commun.* **184** 986 (*Preprint* arXiv:1110.1499 [hep-ph])
[8] Badger S, Biedermann B, Uwer P and Yundin V 2013 *Comput. Phys. Commun.* **184** 1981 (*Preprint* arXiv:1209.0100 [hep-ph])
[9] Cascioli F, Maierhoefer P and Pozzorini S 2012 *Phys. Rev. Lett.* **108** 111601 (*Preprint* arXiv:1111.5206)

[10] van Hameren A 2009 *JHEP* **0907** 088 (*Preprint* arXiv:0905.1005)
[11] Actis S, Denner A, Hofer L, Scharf A and Uccirati S 2013 *JHEP* **1304** 037 (*Preprint* arXiv:1211.6316 [hep-ph])
[12] Gleisberg T, Hoeche S, Krauss F, Schonherr M, Schumann S, et al. 2009 *JHEP* **0902** 007 (*Preprint* arXiv:0811.4622)
[13] Frixione S and Webber B R 2002 *JHEP* **0206** 029 (*Preprint* hep-ph/0204244)
[14] Hoeche S, Krauss F, Schonherr M and Siegert F 2012 *JHEP* **1209** 049 (*Preprint* arXiv:1111.1220)
[15] Hoeche S, Krauss F, Schonherr M and Siegert F 2013 *Phys. Rev. Lett.* **110** 052001 (*Preprint* arXiv:1201.5882)
[16] Gehrmann T, Hoeche S, Krauss F, Schonherr M and Siegert F 2013 *JHEP* **1301** 144 (*Preprint* arXiv:1207.5031)
[17] Hoeche S, Krauss F, Schonherr M and Siegert F 2013 *JHEP* **1304** 027 (*Preprint* arXiv:1207.5030)
[18] Cascioli F, Hoeche S, Krauss F, Maierhofer P, Pozzorini S and Siegert F *Preprint* arXiv:1309.0500 [hep-ph]
[19] ATLAS Collaboration, Aad G et al. 2012 *Phys. Lett.* B **716** 1–29 (*Preprint* arXiv:1207.7214)
[20] CMS Collaboration, Chatrchyan S et al. 2012 *Phys. Lett.* B **716** 30–61 (*Preprint* arXiv:1207.7235)
[21] Ohnemus J 1991 *Phys. Rev.* D **44** 1403–1414
[22] Frixione S 1993 *Nucl. Phys.* B **410** 280–324
[23] Ohnemus J 1994 *Phys. Rev.* D **50** 1931–1945 (*Preprint* hep-ph/9403331)
[24] Dixon L J, Kunszt Z and Signer A 1999 *Phys. Rev.* D **60** 114037 (*Preprint* hep-ph/9907305)
[25] Campbell J M and Ellis R K 1999 *Phys. Rev.* D **60** 113006 (*Preprint* hep-ph/9905386)
[26] Campbell J M, Ellis R K and Williams C 2011 *JHEP* **1107** 018 (*Preprint* arXiv:1105.0020)
[27] Frixione S, Nason P and Oleari C 2007 *JHEP* **0711** 070 (*Preprint* arXiv:0709.2092)
[28] Melia T, Nason P, Rontsch R and Zanderighi G 2011 *JHEP* **1111** 078 (*Preprint* arXiv:1107.5051)
[29] Campbell J M, Ellis R K and Zanderighi G 2007 *JHEP* **0712** 056 (*Preprint* arXiv:0710.1832)
[30] Dittmaier S, Kallweit S and Uwer P 2008 *Phys. Rev. Lett.* **100** 062003 (*Preprint* arXiv:0710.1577)
[31] Dittmaier S, Kallweit S and Uwer P 2010 *Nucl. Phys.* B **826** 18–70 (*Preprint* arXiv:0908.4124)
[32] Bredenstein A, Denner A, Dittmaier S and Pozzorini S 2010 *JHEP* **1003** 021 (*Preprint* arXiv:1001.4006 [hep-ph])
[33] Ossola G, Papadopoulos C G and Pittau R 2007 *Nucl. Phys.* B **763** 147–169 (*Preprint* hep-ph/0609007)
[34] Hahn T 2001 *Comput. Phys. Commun.* **140** 418-431 (*Preprint* hep-ph/0012260)
[35] Denner A, Dittmaier S and Hofer L *in preparation*
[36] Denner A and Dittmaier S 2003 *Nucl. Phys.* B **658** 175–202 (*Preprint* hep-ph/0212259)
[37] Denner A and Dittmaier S 2006 *Nucl. Phys.* B **734** 62–115 (*Preprint* hep-ph/0509141)
[38] Denner A and Dittmaier S 2011 *Nucl. Phys.* B **844** 199–242 (*Preprint* arXiv:1005.2076)
[39] Draggiotis P, Garzelli M, Papadopoulos C and Pittau R 2009 *JHEP* **0904** 072 (*Preprint* arXiv:0903.0356)
[40] Cascioli F, Maierhoefer P, Moretti N, Pozzorini S and Siegert F *Preprint* arXiv:1309.5912 [hep-ph]
[41] Denner A, Dittmaier S, Roth M and Wieders L 2005 *Nucl. Phys.* B **724** 247–294 (*Preprint* hep-ph/0505042)
[42] Lai H L, Guzzi M, Huston J, Li Z, Nadolsky P M, et al. 2010 *Phys. Rev.* D **82** 074024 (*Preprint* arXiv:1007.2241)